Journal of The Electrochemical Society, **149** (5) E143-E147 (2002)
0013-4651/2002/149(5)/E143/5/$7.00 © The Electrochemical Society, Inc.

Dopants in Diamond Nanoparticles and Bulk Diamond

Density Functional Study of Substitutional B, N, P, SB, S, PN, O, NN, and Interstitial H

Titus V. Albu,[a] Alfred B. Anderson,[a,z] and John C. Angus[b,*]

[a]*Department of Chemistry,* [b]*Department of Chemical Engineering, Case Western Reserve University, Cleveland, Ohio 44106, USA*

We show how calculated ionization potentials and electron affinities of doped diamond nanoparticles can be used to predict the donor and acceptor excitation energies of doped n-type and p-type semiconducting bulk diamond. The method uses good quality quantum chemical calculations on small clusters of diamond and doped diamond. Excitation energies are calculated based on differences in total energies of neutral and positively or negatively charged clusters. When charges are free in the bulk, as for an electron associated with substitutional B^-, a simple particle-in-a-box kinetic energy of cluster confinement is taken into account. Optical and thermal excitation energies are calculated for dopants using the B3LYP hybrid density functional method with the 6-31G basis set and substituted $C_{44}H_{42}$ nanocrystals in the bulk structure and with structure optimization around the defects. Based on eight experimentally determined values, the errors of this method are 0.6 eV and less. Calculations at this level allow screening for potential shallow donor and shallow acceptor defects. A classical approach to estimating the cluster confinement energy based on charging the cluster in a polarized dielectric continuum is tested and shown to be less successful.
 [DOI: 10.1149/1.1459681]

Manuscript submitted October 11, 2001; revised manuscript received January 7, 2002. This was Paper 1347 presented at the San Francisco, California, Meeting of the Society, September 2-7, 2001. Available electronically March 22, 2002.

Diamond films grown by chemical vapor deposition are finding uses as inert electrodes.[1-4] When heavily doped with boron, which has a charge carrier activation energy of 0.37 eV at low concentrations, such films are semimetallic.[5,6] Doped diamond films have promise for use in semiconductor devices if sufficiently shallow acceptor and donor dopants can be found.

To assist in the discovery of shallow dopants, quantum theory can be called upon. A successful theoretical approach should allow testing single and multiple atom substitutional and interstitial defects for their donor and acceptor activation energies for generating, respectively, electron (e^-) or hole (h^+) charge carriers. The holes will be at the top of the bulk diamond valence band or at the top of a filled defect band in the bulk diamond bandgap. The electrons will be at the bottom of the bulk diamond conduction band or at the bottom of an empty defect band in the bulk diamond bandgap.

There have been density functional band calculations of bandgap orbital energies that have been used to describe donor and acceptor charge carrier activation energies.[7-11] These permit only rough conclusions to be drawn in part because the orbital eigenenergies do not well represent the bandgap in the Koopmans' sense.[12] Tentative conclusions can also be drawn from orbital energies from semiempirical calculations for neutral cluster models of defect sites in diamond.[13-16]

Full self-consistent field calculations of energies of neutral and ionized cluster models of dopant centers should give accurate ionization potentials (*IP*) and electron affinities (*EA*) of the clusters and provide a route to calculating dopant excitation energies. This approach does not seem to have been pursued, probably because it produces bandgaps that are too large for the bulk. However, as shown below, extrapolation to bulk excitation energies is possible. For the present case, the cluster is a diamond nanocrystal terminated by C-H bonds just like a hydrogenated diamond surface. The lowest optical bandgap excitation creates a state with an electron removed from the top of the crystal filled band and placed in the bottom of the empty band. In the nanocrystal, the electron and hole are trapped close to each other. In bulk diamond, an electron and hole created by bandgap excitation can be fully delocalized and free from each other. The excitation energy for the nanocrystal will be different from that of bulk diamond because of this. When viewing the nanocrystal as a model for the bulk, it is possible to correct for the electron and hole proximity by calculating the cluster *IP* and *EA* and noting that, to this level of approximation, the bulk bandgap, $\Delta E'_B$, is given as

$$\Delta E'_B = E(C_XH_Y^+) + E(C_XH_Y^-) - 2E(C_XH_Y) \quad [1]$$

where the right hand side has total energies of positive, negative, and neutral clusters made up of X carbon and Y hydrogen atoms. Thus, the electron and hole are modeled by being on different noninteracting clusters. The prime is written because a charge confinement energy must also be taken into consideration.

Acceptor excitation energies, $\Delta E'_A$, and donor excitation energies, $\Delta E'_D$, can be similarly calculated to the same level of approximation by the formulas

$$\Delta E'_A = E(AC_{X'}H_Y^-) + E(C_XH_Y^+) - E(AC_{X'}H_Y) - E(C_XH_Y) \quad [2]$$

and

$$\Delta E'_D = E(DC_{X'}H_Y^+) + E(C_XH_Y^-) - E(DC_{X'}Y_Y) - E(C_XH_Y) \quad [3]$$

where, for interstitial acceptors A and donors D, $X' = X$; for substitutional dopants, $X' \neq X$.

Corrections to $\Delta E'_B$ take into account the destabilizations of the electron in $C_XH_Y^-$ and hole in $C_XH_Y^+$ that are caused by their confinement. Ideally, one would increase the cluster sizes until the bulk limit is reached, but that is computationally prohibited. For modeling the corrections, two approaches come to mind: classical and quantum mechanical. Both should lower the energies of the clusters used to model delocalized charge carriers. Let the destabilizations for confining the electron and hole be E_{ce} and E_{ch}, respectively. Then to this level of approximation, Eq. 1 for the bulk bandgap becomes

$$\Delta E_B = E(C_XH_Y^+) + E(C_XH_Y^-) - 2E(C_XH_Y) - E_{ce} - E_{ch} \quad [4]$$

Taking the quantum mechanical viewpoint first, donor excitation energies will be reduced by the confinement energy of the electron in the $C_XH_Y^-$ cluster. The hole should be localized on the donor and the surrounding carbon atoms will be polarized to reduce the posi-

* Electrochemical Society Fellow.
z E-mail: aba@po.cwru.edu

tive charge on it. Enlarging the cluster is assumed to not stabilize the ionized $DC_{X'}H_Y$ cluster relative to the neutral one significantly. Therefore, the donor excitation energy in Eq. 3 becomes

$$\Delta E_D = E(DC_{X'}H_Y^+) + E(C_XH_Y^-) - E(DC_{X'}H_Y) - E(C_XH_Y) - E_{qce} \quad [5]$$

where E_{qce} is calculated quantum mechanically using a model potential.

Acceptor excitation energies will be reduced by the confinement energy of the hole in the $C_XH_Y^+$ cluster. The promoted electron that is associated with the acceptor will be bonded to it weakly, for example, by an electron pairing energy with no coulomb component in the case of the substitutional boron atom. Assuming that this weakly held electron will be described by an orbit considerably larger than that of the $AC_{X'}H_Y$ cluster, the acceptor excitation energy of Eq. 2 becomes

$$\Delta E_A = (AC_{X'}H_Y^+) + E(C_XH_Y^-) - E(AC_{X'}H_Y) - E(C_XH_Y) - E_{qce} - E_{qch} \quad [6]$$

where E_{qch}, the hole confinement energy, is evaluated similarly to E_{qce}.

The classical approach used is that of correcting the energies of all charged clusters by calculating their interaction with a polarized surround with the diamond dielectric constant.[17] The polarized continuum model, outlined in the documentation to the Gaussian 98 quantum chemistry package of Ref. 17 is essentially related to the Born model originally used for estimating solvation energies of ions.[18] In this approach, a stabilization energy is added to all of the charged cluster energies in Eq. 1-3.

The results of these two approaches will be seen to have remarkable similarities in donor excitation energies. However, the classical approach significantly overestimates the bandgap and B acceptor excitation energy and is in poorer agreement with all results on the physical scale.

Tables of excitation energies quickly convey information that is used in formulas for semiconductor charge carrier concentrations where excitations are thermally or photoinduced. Other important physical properties such as space charge formation and band bending at interfaces depend on *IP*s and *EA*s of materials on either side of the interface and these properties are reported relative to the vacuum level, which is zero on the physical scale. Bulk *IP*s based on clusters are calculated by

$$IP = E(\text{positive cluster}) + E(e^-) - E(\text{cluster}) - E_{ce} \quad [7]$$

where the electron is at the vacuum level such that $E(e^-) = 0$. Bulk electron affinities based on clusters are calculated by

$$-EA = E(\text{negative cluster}) - E(\text{cluster}) - E(e^-) + E_{ch} \quad [8]$$

where the electron comes from the vacuum level and the negative sign on *EA* gives the convention that a material that attracts electrons from the vacuum level has a positive *EA*. A general schematic illustration of donor and acceptor energies and bandedges is in Fig. 1. In the case of some diamond surfaces, *EA* is negative and the CB edge in Fig. 1 would then lie above the vacuum level.

Computational Approach

The hydrogen terminated $C_{44}H_{42}$, $XC_{43}H_{42}$, and $XYC_{42}H_{42}$ clusters are used with CH internuclear distances fixed at 1.11 Å, and all unrelaxed CC internuclear distances fixed at the bulk bond length, 1.5445 Å. Figure 2 shows the carbon atom framework with shaded circles indicating the atoms that are allowed to relax. The lower diagram defines the directions along which the shaded atoms are allowed to relax and specifies the positions of substitutional dopant atoms X and Y.

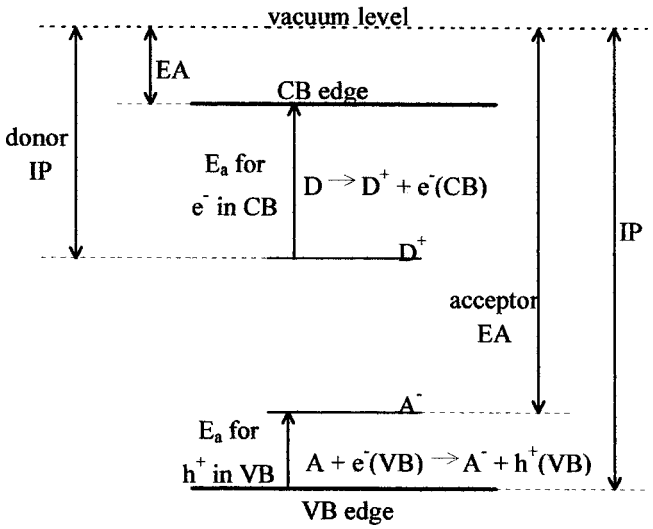

Figure 1. Schematic state energy diagram showing relationships between a semiconductor conduction band (CB) edge, valence band (VB) edge, donor (D) ionization potential (*IP*), acceptor (A), electron affinity (*EA*), and activation energies (E_a).

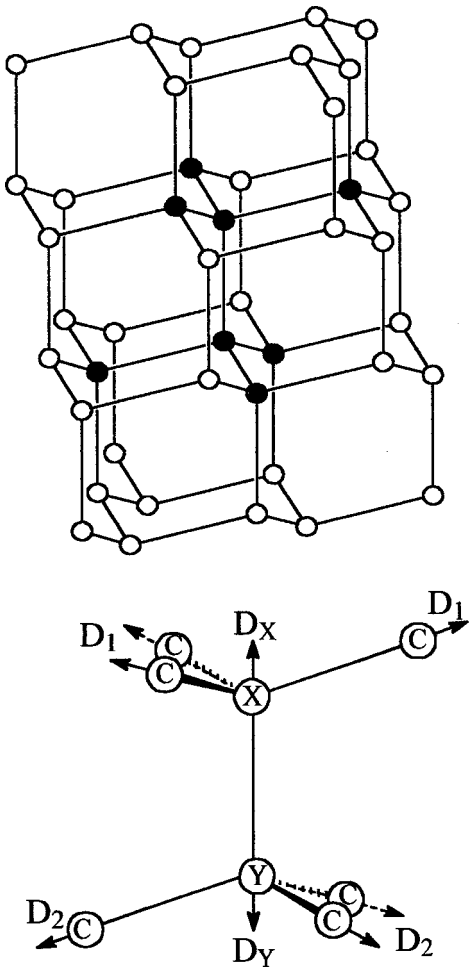

Figure 2. $C_{44}H_{42}$ cluster used in the calculations with H not shown. The shaded atoms are those in the lower diagram. Positions of these eight atoms were relaxed in the calculations. Arrows indicate axes along which relaxation was permitted, and as drawn correspond to positive values of displacement. X and Y represent substitutional dopant atoms.

Table I. Internuclear distances (Å) based on B3LYP/6-31G calculations with structure relaxations as in Fig. 1.

Defect	Charge	Formula	X	D_X	D_1	Y	D_Y	D_2
Nonsubstitutional	0	$C_{44}H_{42}$	C	0.003	0.020	C	0.003	0.020
	+1	$C_{44}H_{42}^+$	C	0.045	0.015	C	0.045	0.015
	−1	$C_{44}H_{42}^-$	C	0.002	0.021	C	0.002	0.021
P substitutional	0	$C_{43}PH_{42}$	P	−0.005	0.166	C	0.160	0.051
	+1	$C_{43}PH_{42}^+$	P	−0.004	0.166	C	0.159	0.049
S, B substitutional	0	$C_{42}SBH_{42}$	S	0.044	0.255	B	0.186	0.070
	+1	$C_{42}SBH_{42}^+$	S	−0.027	0.188	B	0.236	0.076
N substitutional	0	$C_{43}NH_{42}$	N	0.207	0.022	C	0.231	0.021
	+1	$C_{43}NH_{42}^+$	N	0.004	0.045	C	0.027	0.022
S substitutional	0	$C_{43}SH_{42}$	S	0.297	0.251	C	0.168	0.025
	+1	$C_{43}SH_{42}^+$	S	0.068	0.195	C	0.351	0.046
P, N substitutional	0	$C_{42}PNH_{42}$	P	0.023	0.173	N	0.543	0.050
	+1	$C_{42}PNH_{42}^+$	P	0.074	0.176	N	0.278	0.062
O substitutional	0	$C_{43}OH_{42}$	O	−0.054	0.204	C	0.120	0.024
	+1	$C_{43}OH_{42}^+$	O	−0.042	0.188	C	0.106	0.026
2N substitutional	0	$C_{42}N_2H_{42}$	N	0.305	0.014	N	0.305	0.014
	+1	$C_{42}N_2H_{42}^+$	N	0.205	0.033	N	0.205	0.033
H interstitial[a]	0	$C_{44}H_{43}$	C	0.328	0.047	C	0.328	0.047
	+1	$C_{44}H_{43}^+$	C	0.298	0.050	C	0.298	0.050
B substitutional	0	$C_{43}BH_{42}$	B	0.120	0.054	C	0.115	0.020
	−1	$C_{43}BH_{42}^-$	B	0.005	0.049	C	0.030	0.019

[a] H atom is assumed equally distanced between the atoms X and Y.

Hybrid density functional theory calculations were performed using the B3LYP method with a 6-31G atomic basis set. Comparisons with other basis sets showed that this one was cost effective in terms of computer time, and sufficiently accurate compared to much slower extended basis set calculations. The Gaussian 98 software was used.[17] When calculating the effects of the dielectric surround on cluster charging, the simple polarized continuum model option of Gaussian 98 was employed. A default value of 5.621 was used for the dielectric constant, which approximates the diamond value of 5.5.

The $XYC_{42}H_{42}$ clusters measure approximately $6.8 \times 6.8 \times 9.2$ Å. The energy of a particle of mass m in a box is given by

$$E_{n_x n_y n_z} = \frac{\hbar^2 \pi^2}{2m}\left(\frac{n_x^2}{L_x^2} + \frac{n_y^2}{L_y^2} + \frac{n_z^2}{L_z^2}\right) \quad [9]$$

For an electron in its ground state ($n_x = n_y = n_z = 1$) in this box ($L_x = L_y = 6.8$ Å and $L_z = 9.2$ Å) the energy is 2.07 eV. Effective mass approximations for electrons and holes that are used in theoretical interpretations of bulk electronic properties break down when applied to very small nanoparticles.[19-21] Setting the quantum confinement energies for the electron and the hole, E_{qce} and E_{qch}, both equal to the free electron mass energy value of 2.07 eV, results in good agreement with available experimental data. A few calculations have also been made using a larger $XYC_{96}H_{78}$ cluster.[22] Its dimensions, determined in the same way as for the smaller cluster, were $9.6 \times 9.6 \times 9.2$ Å for which the quantum confinement energy is 1.26 eV. However, this was too small to give the experimental bandgap (5.49 eV). Increasing E_{ce} and E_{ch} to 1.65 eV did yield the experimental gap and good predictions for several donor excitation energies. Thus, the quantum confinement energy could be viewed as a semiempirical parameter.

Results

Quantum corrected excitation energies.—As explained earlier, the calculated electronic properties reported herein are derived from calculations of *IP*s and *EA*s of nanocrystals of diamond and doped diamond nanocrystals with approximate quantum or classical extrapolations. The results of the more accurate quantum approach are given first; these results and the $XYC_{96}H_{78}$ results are discussed in greater detail elsewhere.[22]

As may be seen in Table I, there are large structure changes upon ionization of some of the doped clusters. When N substitutes for C in the diamond lattice, an extra electron is introduced and it has to occupy an orbital in the antibonding (σ^*) conduction band. When a C-N bond is stretched, a σ^* orbital directed along the stretched bond becomes stabilized and drops, bearing one electron into the bandgap. The N-C bond order is then $\frac{1}{2}$ and the bond stretches as far as the restoring forces due to the neighboring carbon atoms and further neighbors in the lattice let it. The bond stretches 0.44 Å from the bulk value. Upon ionization, the σ^* orbital is empty and the restoring forces from the neighboring atoms push the N-C bond to a shorter value, reducing it by 0.41 Å. In the case of N-N, there are two electrons in the σ^* orbital and the N-N bond order is 0 and the

Table II. $-IP$ (eV) for positive ionization products and $-EA$ (eV) for negative ionization products from B3LYP/6-31G total energies of neutral and charged $C_{44}H_{42}$, $XC_{43}H_{42}$, and $XYC_{42}H_{42}$ clusters. The optical column is for the charged cluster with the same structure as the neutral cluster and the thermal column is for the structurally relaxed charged cluster. A quantum confinement correction is included for C^+, B^-, and C^-.

Ionization Product	$-IP$ or $-EA$	
	Optical	Thermal
C^-	0.49	0.49
P^+	−0.53	−0.53
SB^+	−1.30	−1.00
N^+	−2.28	−1.04
S^+	−1.44	−1.04
PN^+	−2.09	−1.28
O^+	−2.62	−2.61
N_2^+	−3.51	−3.05
H^+(i)	−3.35	−3.33
B^-	−4.21	−4.75
C^+	−5.20	−5.12

Table III. HOMO or LUMO energy eigenvalues (eV), from B3LYP/6-31G calculations on $C_{44}H_{42}$, $XC_{42}H_{42}$, and $XYC_{42}H_{42}$ clusters.

Cluster	Orbital	Orbital energy
$C_{44}H_{42}$	LUMO[a]	1.46
$PC_{43}H_{42}$	HOMO[b]	0.58
$SBC_{42}H_{42}$	HOMO	0.00
$NC_{43}H_{42}$	HOMO	−0.90
$SC_{43}H_{42}$	HOMO	−0.23
$PNC_{42}H_{42}$	HOMO	−0.85
$OC_{43}H_{42}$	HOMO	−1.43
$N_2C_{42}H_{42}$	HOMO	−2.21
$H(i)C_{44}H_{42}$	HOMO	−2.05
$BC_{43}H_{42}$	LUMO	−3.48
$C_{44}H_{42}$	HOMO	−6.03

[a] Lowest unoccupied molecular orbital.
[b] Highest occupied molecular orbital.

N-N internuclear distance is 0.61 Å greater than the C-C distance. Ionizing this bandgap orbital restores a bond order of $\frac{1}{2}$ and the N-N distance decreases by 0.20 to 0.41 Å, which is close to the N-C half-order band length of 0.44 Å. The other donor substitutional atoms and ions can be analyzed similarly. In the case of the substitutional boron acceptor atom, there is one less bonding electron, so a bonding σ orbital from the valence band rises up into the bandgap as a B-C bond of order $\frac{1}{2}$ stretches. The stretch is 0.23 Å and when an electron is added to the boron to create B^-, there is a relaxation of 0.20 Å back to the bulk diamond value since the bond order is restored to 1. By stabilizing the ionized states, these relaxations make the thermal excitation energies smaller than the optical ones.

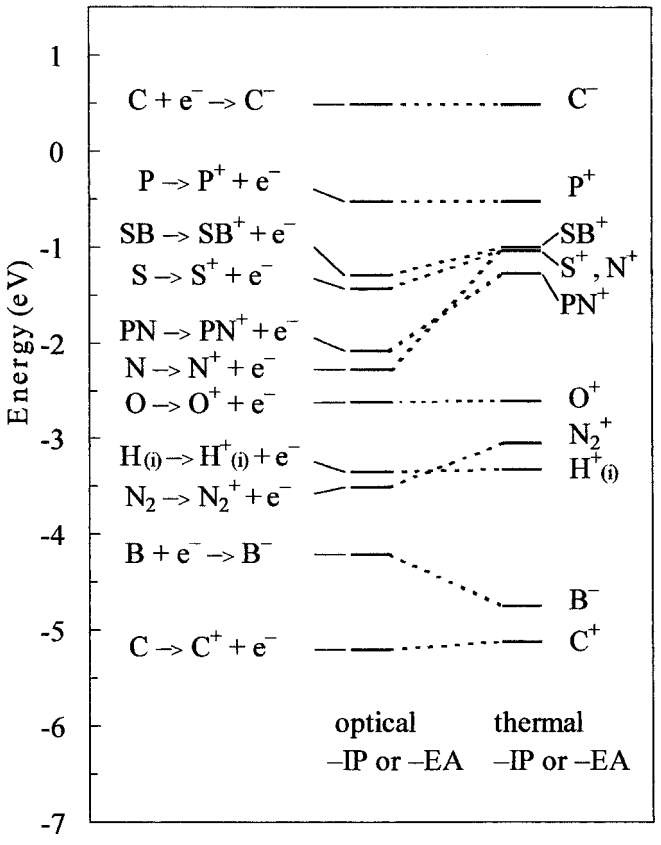

Figure 3. Predicted optical and thermal energies based on cluster IP and EA calculations and including a 2.07 eV quantum confinement energy correction for forming C^+, C^-, and B^-. C stands for $C_{44}H_{42}$, C^+ for $C_{44}H_{42}^+$ etc.; see Table II. The electron energy is zero.

Table IV. Predicted bulk excitation energies (eV) calculated from the cluster results in Table II. Experimental values from the literature are in parentheses for comparison.

	Excitation energy	
Defect	Optical	Thermal
B acceptor	0.99	0.37 (0.37)[a]
P donor	1.02 (0.55)[b]	1.02 (0.46)[c]
SB donor	1.79	1.49
N donor	2.77 (≥2.2)[d]	1.53 (1.60)[e]
S donor	1.93	1.53
PN donor	2.58	1.77
O donor	3.11	3.10
N_2 donor	4.00 (3.8)[f]	3.54
H(i) donor	3.84 (4.1)[g]	3.82

[a] Ref. 23.
[b] Ref. 24.
[c] Ref. 25.
[d] Refs. 26, 27.
[e] Ref. 28.
[f] Ref. 29.
[g] Ref. 30. The authors of Ref. 30 did not assign this hydrogen-induced absorption edge to interstitial H, but, from the above comparison, we are proposing this assignment.

All calculated optical and thermal $-IP$ and $-EA$ for the clusters, the former decreased by $E_{qch} = 2.07$ eV for $C_{44}H_{42}^+$ and the latter increased by $E_{qce} = 2.07$ eV for $C_{44}H_{42}^-$ and $BC_{43}H_{42}^-$, are in Table II. Using negative signs on *IP* and *EA* puts the energies of the states on the physical scale with the vacuum level at $E = 0$. It is emphasized that these are not energies of orbital eigenvalues. The donor or acceptor orbital eigenvalues for the neutral clusters are listed in Table III. They lie ~0.7 to 1.5 eV higher, except for C^+, which is 1.2 V lower.

Results from Table II are displayed in Fig. 3. The ionization energy shifts due to relaxation are clearly evident within the bandgap. The bandgap itself, 5.61 eV, is close to the measured value of 5.49 eV. Predicted optical and thermal excitation energies are in Table IV. Of the seven comparisons with experiment that are given (not including the bandgap prediction just mentioned), the largest error is 0.6 eV.[23-30]

Classically corrected excitation energies.—The polarized continuum calculations yield stabilizations of $C_{44}H_{42}^-$ and $BC_{43}H_{42}^-$ clus-

Table V. $-IP$ (for positive species) or $-EA$ (for negative species) from B3LYP/6-31G total energies of neutral and charged clusters. See caption to Table II. The classical corrections for cluster charging energies are used as discussed in the text. Units are in electronvolts.

	$-IP$ or $-EA$	
Ionization Product	Optical	Thermal
C^-	1.53	1.53
P^+	0.56	0.56
SB^+	−0.21	0.09
N^+	−1.19	0.01
S^+	−0.35	0.05
PN^+	−1.00	−0.19
O^+	−1.53	−1.52
N_2^+	−2.42	−1.96
$H^+(i)$	−2.26	−2.24
B^-	−3.18	−3.72
C^+	−6.22	−6.14

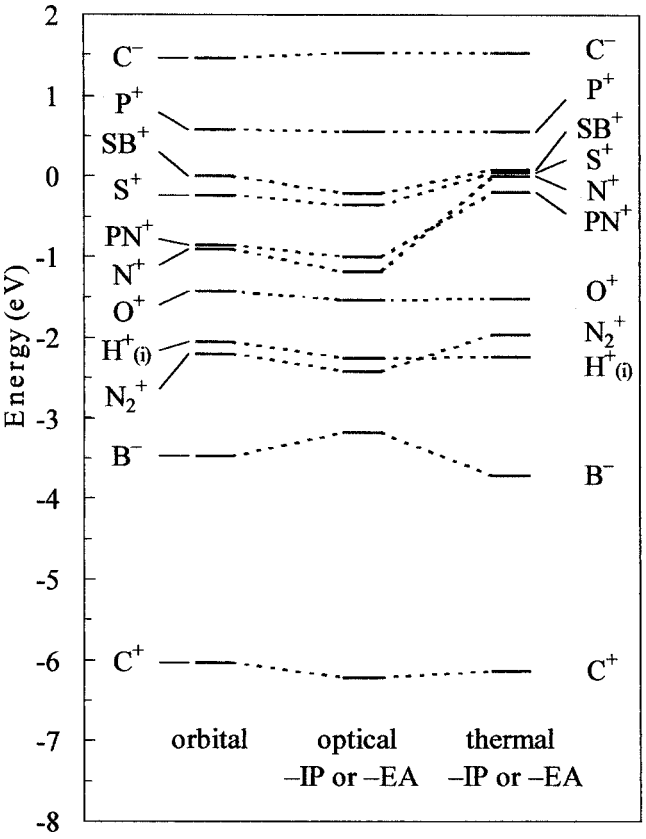

Figure 4. As in Fig. 3, but using the classical corrections to predict optical and thermal energies and including the HOMO (donor) energy levels for donors and LUMO (acceptor) energy levels for acceptors obtained in neutral cluster calculations.

ters by 1.03 and 1.04 eV, respectively. $C_{44}H_{42}^{+}$ and $NC_{43}H_{42}^{+}$ are stabilized by 1.05 and 1.09 eV, respectively. The 1.09 eV stabilization is assumed for the other positively charged doped clusters as well. Table V gives resulting $-IP$ and $-EA$ values for all of the nanocrystals with contributions due to the dielectric surround approximations included.

The bandgap, 7.71 eV, is 2.24 eV too large and the substitutional B excitation energy is 2.09 eV too large but all other predictions (Table IV) are very close to those obtained using the quantum confinement correction. This is because the dielectric-surround model-induced 1.03 eV increase in $C_{44}H_{42}$ *EA* and 1.09 eV decrease in the $XYC_{42}H_{42}$ *IP* brings all donors 2.12. eV closer to the conduction band. This is about the same as the quantum confinement correction on $C_{44}H_{42}^{-}$ bringing the conduction band 2.07 eV closer to the uncorrected donors. However, the dielectric correction gives only about half of the needed decrease in cluster bandgap and half of the needed decrease in substitutional B excitation energy. The electronic structures based on this model are in Fig. 4 along with the B3LYP highest occupied or lowest unoccupied orbital energies for the neutral nanocrystals. Interestingly, the orbital energies and the excitation energies are in rather good agreement with one another. Comparison with more accurate quantum confinement based predictions in Fig. 3 brings out the above-mentioned deficiencies in the classical confinement approach.

Conclusions

It has been shown how to estimate doped bulk diamond electronic properties based on doped nanocluster *IP* and *EA*s together with energy contributions based on spatial confinement of the added charge. The quantum confinement energies, based on the particle-in-a-box model yield more accurate bulk predictions than the classical model for charging the nanoclusters in a polarized dielectric continuum. Compared with eight pieces of experimental data, the largest error in the quantum approach is 0.6 eV.

Acknowledgment

This research is supported by the U.S. National Science Foundation, grant no. CHE-9816345.

Case Western Reserve University assisted in meeting the publication costs of this article.

References

1. G. M. Swain, A. B. Anderson, and J. C. Angus, *MRS Bull.*, **23**, 56 (1998).
2. R. Tenne and C. Levy Clement, *Isr. J. Chem.*, **38**, 57 (1998).
3. Y. V. Pleskov, *Russ. Chem. Rev.*, **68**, 381 (1999).
4. J. C. Angus, H. B. Martin, U. Landau, Y. E. Evstefeeva, B. Miller, and N. Vinocur, *New Diamond Front. Carbon Technol.*, **9**, 175 (1999).
5. R. J. Zhang, S. T. Lee, and Y. W. Lam, *Diamond Relat. Mater.*, **5**, 1288 (1996).
6. M. Werner and R. Locher, *Rep. Prog. Phys.*, **61**, 1665 (1998).
7. S. A. Kajihara, A. Antonelli, J. Bernholc, and R. Car, *Phys. Rev. Lett.*, **66**, 2010 (1991).
8. P. Briddon, R. Jones, and G. M. S. Lister, *J. Phys. C*, **21**, L1022 (1988).
9. S. Poykko, M. Kaukonen, M. J. Puska, and R. M. Nieminen, *Comput. Mater. Sci.*, **10**, 351 (1998).
10. D. Saada, J. Adler, and R. Kalish, *Appl. Phys. Lett.*, **77**, 878 (2000).
11. T. Miyazaki and H. Okushi, *Diamond Relat. Mater.*, **10**, 449 (2001).
12. C. Y. Fong and B. M. Klein in *Diamond: Electronic Properties and Applications*, L. S. Pan and D. R. Kania, Editors, p. 1, Kluwer Academic Publishers, Boston (1995).
13. A. B. Anderson and S. P. Mehandru, *Phys. Rev. B*, **48**, 4423 (1993).
14. S. P. Mehandru and A. B. Anderson, *J. Mater. Res.*, **9**, 383 (1993).
15. A. B. Anderson, E. J. Grantscharova, and J. C. Angus, *Phys. Rev. B*, **54**, 14341 (1996).
16. A. B. Anderson and L. N. Kostadinov, *J. Appl. Phys.*, **81**, 264 (1997).
17. M. J. Frisch, G. W. Trucks, H. B. Schlegel, G. E. Scuseria, M. A. Robb, J. R. Cheeseman, V. G. Zakrewski, J. A. Montgomery, R. E. Stratmann, J. C. Burant, S. Dapprich, J. M. Millam, A. D. Daniels, K. N. Kudin, M. C. Strain, O. Farkas, J. Tomasi, V. Barone, M. Cossi, R. Cammi, B. Mennucci, C. Pomelli, C. Adamo, S. Clifford, J. Ochterski, G. A. Petersson, P. Y. Ayala, Q. Cui, K. Morokuma, D. K. Malick, A. D. Rabuck, K. Raghavachari, J. B. Foresman, J. Cioslowski, J. V. Ortiz, B. B. Stefanov, G. Liu, A. Liashenko, P. Piskorz, I. Komaromi, R. Gomperts, R. L. Martin, D. J. Fox, T. Keith, M. A. Al-Laham, C. Y. Peng, A. Nanayakkara, C. Gonzalez, M. Challacombe, P. M. W. Gill, B. G. Johnson, W. Chen, M. W. Wong, J. L. Andres, M. Head-Gordon, E. S. Replogle, and J. A. Pople, *Gaussian 98*, Revision A.1, Gaussian, Inc., Pittsburgh, PA (1998).
18. P. W. Atkins, *Physical Chemistry*, 6th ed., p. 246, W. H. Freeman, New York (1998).
19. L. E. Brus, *J. Chem. Phys.*, **80**, 4403 (1984).
20. Y. Wang, A. Suna, W. Muhler, and R. Kasowksi, *J. Chem. Phys.*, **87**, 7315 (1987).
21. F. W. Wise, *Acc. Chem. Res.*, **33**, 773 (2000).
22. T. V. Albu, A. B. Anderson, and J. C. Angus, To be published.
23. R. Kalish, A. Reznik, C. Uzan-Saguy, and C. Cyterman, *Appl. Phys. Lett.*, **76**, 757 (2000).
24. M. Nesladek, K. Meyhens, K. Haenen, L. M. Stals, T. Terqje, and S. Koizumi, *Diamond Relat. Mater.*, **8**, 882 (1999).
25. S. Kaizumi, M. Kamo, Y. Sato, S. Mita, A. Sawabe, A. Reznik, C. Uzan-Saguy, and R. Kalish, *Diamond Relat. Mater.*, **8**, 882 (1998).
26. H. B. Dyer, R. A. Roal, L. D. Preez, and J. H. N. Loubser, *Philos. Mag.*, **11**, 763 (1965).
27. J. Rosa, M. Vanecek, M. Nesladek, and L. M. Stals, *Diamond Relat. Mater.*, **8**, 721 (1999).
28. R. G. Farrer, *Solid State Commun.*, **7**, 685 (1969).
29. G. Davies, *J. Phys. C*, **9**, L537 (1976).
30. J. Ristein, W. Stein, and L. Ley, *Phys. Rev. Lett.*, **78**, 1803 (1997).